# Supporting Information for:

## "Proton exchange membrane with plasmon-active surface for enhancement of fuel cell effectivity"

by

R. Elashnikov[a], K. Zahorjanova[a], E. Miliutina[a], Z. Kolska[b] M. Cieslar[c], V. Svorcik[a], O. Lyutakov[a]

[a] *Department of Solid State Engineering, University of Chemistry and Technology, 16628 Prague, Czech Republic*

[b] *Faculty of Science, J.E. Purkyne University, 400 96 Usti nad Labem, Czech Republic*

[c] *Faculty of Mathematics and Physics, Charles University, 121 16 Prague, Czech Republic*

## Experimental

### Materials and samples preparation

PEM membrane (Nafion Membrane NR 212, 50.8 µm) was supplied from Ion Power. The conductivity of the surface of PEM membrane was increased by the deposition of thin porous amorphous carbon layer ("effective" thickness – ca 7 nm) using flash evaporation method (BAL-TEC). Next, Au clusters were deposited onto a PEM/C surface by vacuum sputtering (99.999 Au target purity (Safina), DC Ar plasma, gas pressure 4 Pa, discharge power of 7.5 W). The sputtering time (20 s) was adjusted to create the Au clusters and prevent the formation of continuous Au layer. Then, a thin Pt layer was deposited on the PEM/C/Au surface (in particular on Au clusters surface) by samples immersion into 10 mM water solution of $H_2PtCl_6$(Sigma-Aldrich),followed by drop wise addition of 100 mM water solution of ascorbic acid (Sigma Aldrich) with gentle mixing (volume ratio of solutions is 2.5:1, respectively). After Pt deposition the samples were carefully rinsed with distilled water and methanol and dried at the ambient conditions.

Commercially available fuel cells from (Horizon – Fuel Cell Technology) was used to test 4 $cm^2$ active-area PEM/C/Au/Pt membrane. The supplied fuel cell station design was modified to introduce the light triggering: the set-up for PEM membrane mounting was replaced by home-made one with the addition of a transparent glass (BK7). In turn, the PEM membrane from manufacturer was replaced by laboratory-prepared PEM/C/Au/Pt membrane. The supply of hydrogen and oxygen as well as control of the membrane moisture were carried out on the basis of the manufacturer's devices. The gases feed rate was7 mL·min$^{-1}$for hydrogen and 3.5 mL·min$^{-1}$ for oxygen (controlled with the use of equipment from the fuel cell station station). The current and voltage produced by the set-up were measured by a voltammeter, supplied as an integral part of the station kit. The cell polarisation and power density curves were determined from current/voltage relationship (measured by multimeters) under the fuel cell loading with different resistors.

The light triggering was performed using the LED light source (780 nm emission wavelength, maximal power – 500 mW). The LED light was collimated on the PEM/C/Au/Pt membrane surface in the spot with 1.5 cm diameter through a transparent window (see Fig. 1 schematic representation of set-up).

*Measurement techniques*

X-ray photoelectron spectroscopy (XPS) was performed using an Omicron Nanotechnology ESCAProbeP spectrometer fitted with a monochromated Al Kα X-ray source working at 1486.6 eV. Surface morphology was measured using atomic force microscopy (AFM) in peak force mode on the Icon (Bruker) microscope. AFM scratch tests were carried out on Au or Au/Pt films deposited on the glass substrate by profiling across a scratch at the angle of 90° relative to the substrate surface. X-ray diffraction data (XRD) were collected on XRD diffractometer PANanalytical X'Pert PRO using Cu Kα radiation (1.5406 Å). All spectra are presented after baseline correction and subtraction of the spectrum from previous sample preparation stage (i.e. subtraction the spectrum of PEM/C/Au from spectrum of PEM/C/Au/Pt). UV–Vis absorption spectra were measured by using a Lambda 25 UV–vis–NIR spectrometer (PerkinElmer, USA) with the scanning rate of 480 nm min$^{-1}$.To estimate the surface temperature an ultrathin (10 µm) leaf-type thermocouple was attached to the sample surface and the laser beam was focused on the sample surface below the working edge of the thermocouple. The surface area was determined from $N_2$ adsorption and desorption isotherms (Quantachrome Instruments, NOVA3200) using NovaWin software. Five points Brunauer-Emmett-Teller (BET) analysis was applied for the total surface area determination and each sample was measured four times with a relative experimental error of 5 %.

TEM images of nanoparticles were obtained on a JEOL JEM-1010 transmission electron microscope with a SIS MegaView III digital camera. STEM observations and EDX analyses were performed on a JEOL JEM-2200FS electron microscope equipped with a 100 mm$^2$ JEOL Dry SD100GV EDX detector with a Super UTW window.

Proton penetration measurements were performed on the home made equipment, through the immersion of glass tube filled with diluted nitric acid (pH = 4) in the distilled water and clogged from the bottom side by pristine PEM (control experiments) or PEM/C/Au/Pt membranes. The proton penetration was monitored as time-resolved changes of pH in distilled water (under gently stirring) using the Orion Star A211 (Thermo Scientific) pH-meter.

Electrochemical measurements were performed with Palm Sens 4potentiostat (Palm Instruments, Netherlands), controlled by PSTrace 5.3 software (5.3.1127 firmware) using a three-electrode home made cell, which contains the transparent windows for samples illumination. A HydroFlex hydrogen electrode was used as a reference electrode, a thin platinum wire (10 µm

diameter) auxiliary electrode was used as counter electrode and surface modified PEM membranes were used as the working electrode. Parameters of the voltammetry (VA) measurements were: 10 mV·s$^{-1}$ scan rate and 0.3 to 1.2 mV (in the case of ORR) or -0.2 to 0.9 mV (in the case of HOR) potential range. The measurements were performed in 0.1 M KOH solution purged with oxygen (ORR) or hydrogen (HOR) for 20 min. and subsequent measurements were performed at atmospheric pressure under the continuous flow of corresponding gases through the measurement cell.

*Control experiments.* The control experiments include the temperature control (the electric current produced by fuel cell with PEM/C/Au/Pt membrane was estimated at elevated temperature without illumination), light control (the PEM/C/Au/Pt membrane introduced into fuel cell was illuminated with wavelength which does not correspond to plasmon absorption band at 450 nm) and plasmonic control (the PEM membrane surface was decorated only by C and Pt thin layer, according the previously described procedure, introduced in the fuel cell and illuminated at 780 nm).
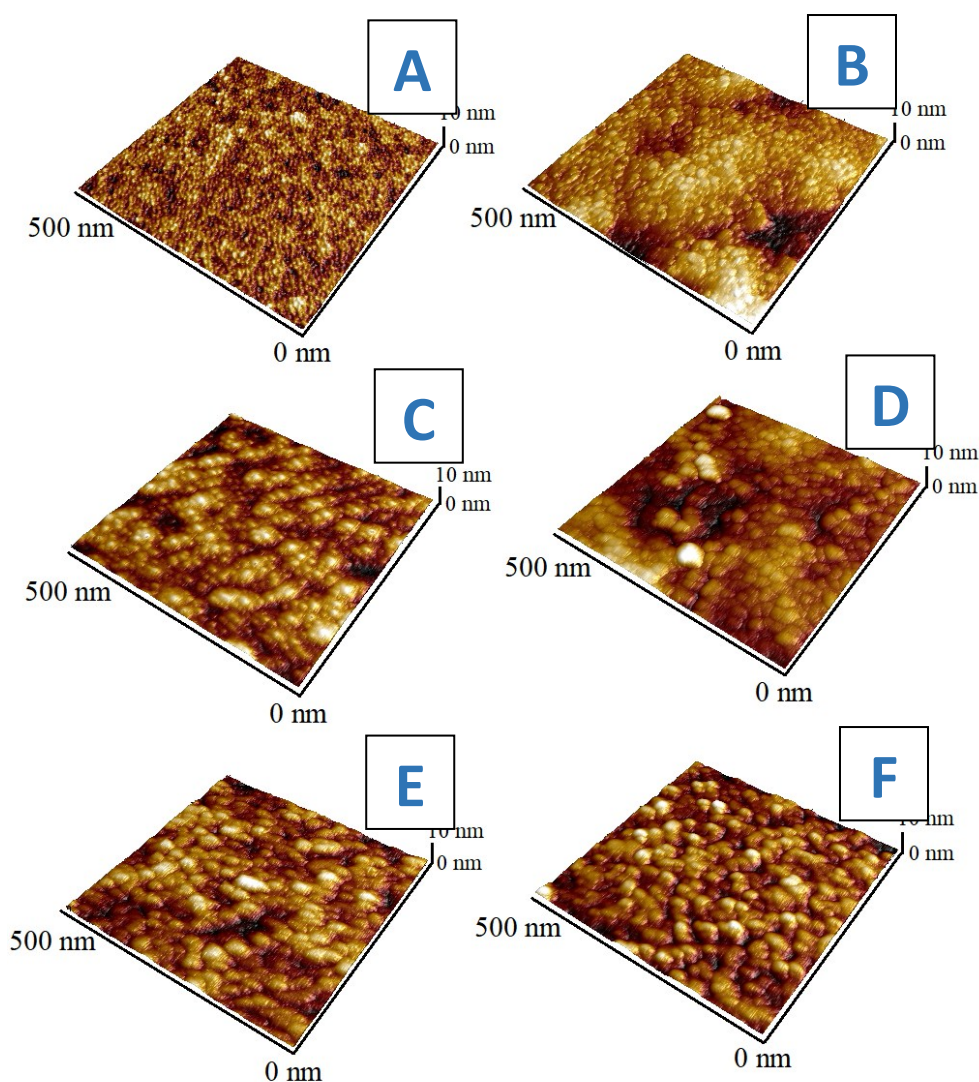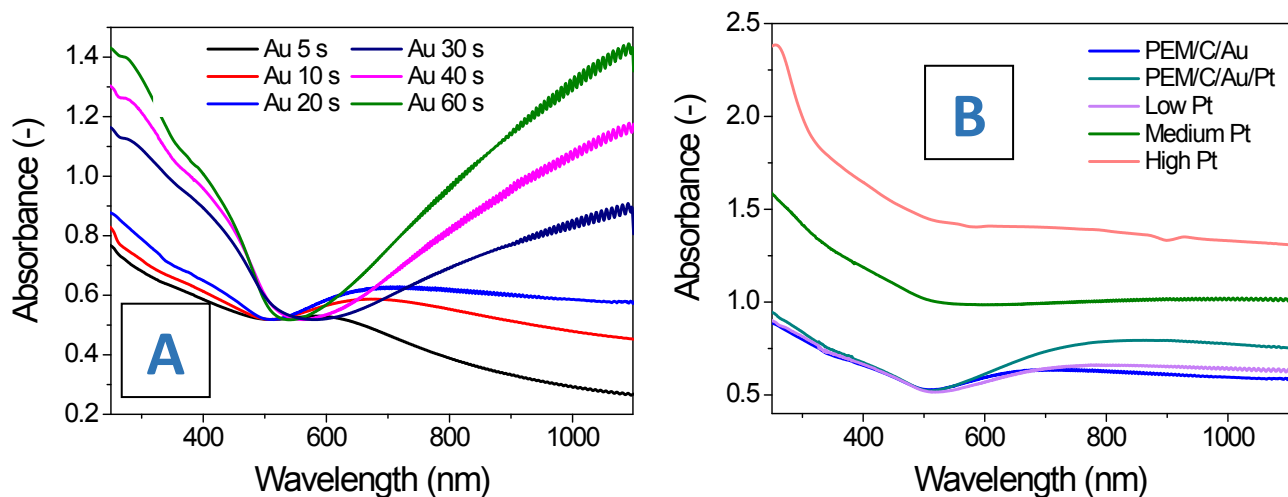
**Figure S1**

Evolution of surface morphology of PEM/C/Au samples during the deposition of Au nanoclusters. The amount of deposited Au was varied using the tuning of depostion time: A – 5 sec (effective thickness – 0.8 nm), B – 10 sec. (effective thickness – 2.6 nm); C – 20 sec. (effective thickness – 7.1 nm); D – 30 sec. (effective thickness – 10.8 nm); E – 40 sec. (effective thickness – 18.3) and F – 60 sec. (effective thickness – 23.8). *

*Effective thickness was estimated from conrol AFM scratch test smesurements using the deposition of Au on glass substrate.
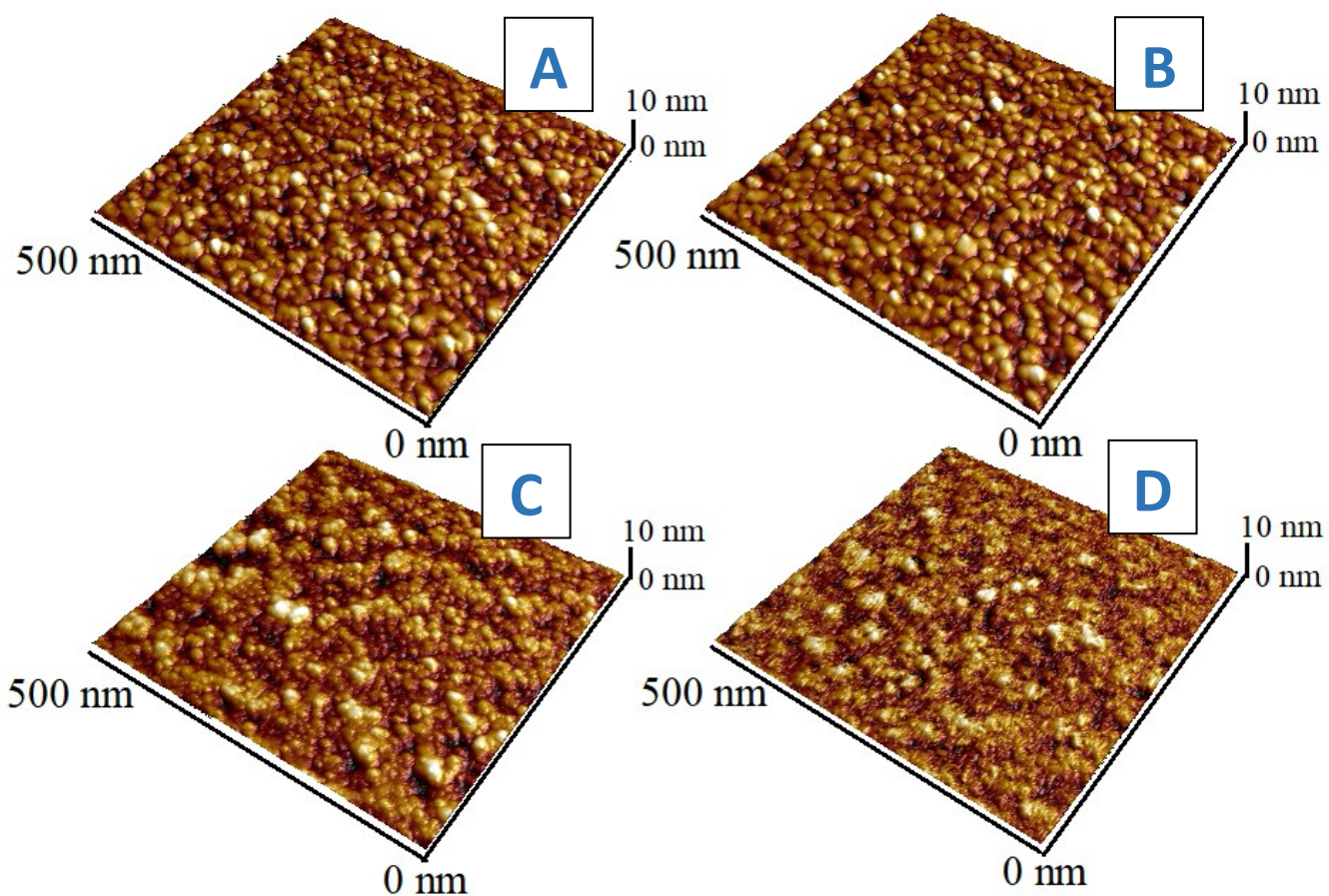
**Figure S2**

Evolution of surface morphology of PEM/C/Au/Pt surface morphology during the addition of different amounts of Pt (tuned by reduction time, estimated from control scratch measurements, are performed on glass/Au supports): A – 0.7 nm; B – 1.2 nm; C – 3.2 nm; D – 7.6 nm.
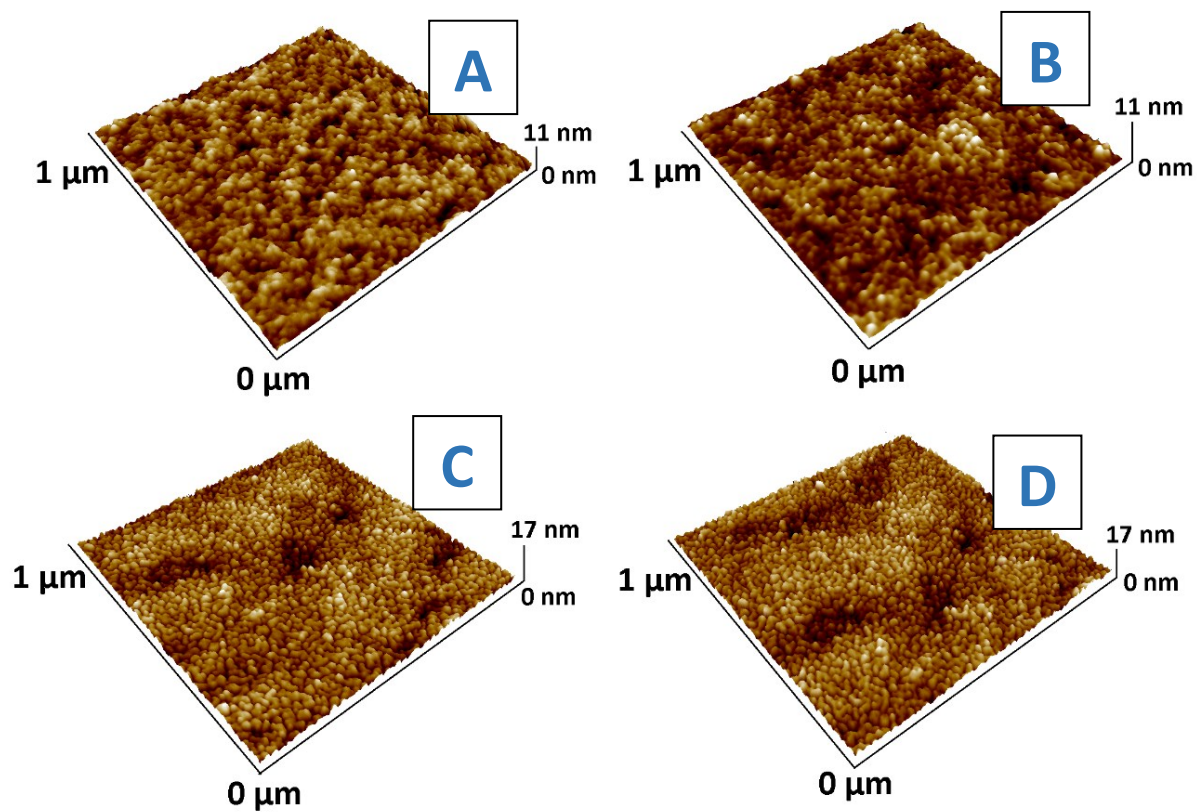
**Figure S3**

UV-Vis spectra of PEM/C/Au membranes with different amount of Au (A), with following effective thicknesses as a function of deposition time: 5 sec – 0.8 nm, 10 sec – 2.6 nm, 20 sec – 7.1 nm, 30 sec. – 10.8 nm, 40 sec – 18.3 nm, 60 sec – 23.8 nm.* (B) – UV-Vis absorption spectra as a function of different amount of Pt (B), deposited on "optimal" Au thickness (7.1 nm).

**Figures S1-S3 – related discussion**

The structure optimization was performed from two points of view: the amount of deposited Au and subsequently deposited Pt. In the first stage, different sputtering times were used for Au deposition. The "effective" gold thickness was estimated from control AFM scratch tests. The surface morphology after the deposition of the different amount of Au was estimated from AFM (Fig. S1), where the formation of a cluster-like structure under the shorter time of deposition is evident. In turn, UV-Vis measurements indicate well visible plasmon resonance after the deposition during 5, 10, and 20 s (Fig. S3A). Further prolongation of deposition time led to clusters conglutination and formation of a continuous Au film with related disappearance of the characteristic plasmon absorption band. Considering the wavelength position and strength of the plasmon absorption band, the 20 s. of Au deposition (effective thickness – 7.1 nm) was chosen for further experiments.

In the second step, we optimized the amount of deposited Pt (AFM measurements of the surface morphology after Pt deposition shows the evolution of optical properties) (Fig. S2, Fig. S3B). As is evident, the deposition of lower Pt content (up to 1,2 nm) does not significantly affect the surface morphology. The corresponded UV-Vis spectra (Fig. S3B) also shows the persistence of the plasmon absorption band, which becomes wider and shifted to NIR range, but is still visible. Oppositely, the increasing of Pt content leads to quenching of plasmon absorption band, due to sticking together of metal clusters (Figs. S2, S3).

**Figure S4**

Results of AFM measurements of PEM/C/Au/Pt surface at the different stages of preparation: A – pristine PEM surface, B – PEM/C surface, C – PEM/C/Au surface, D – PEM/C/Au/pt surface.
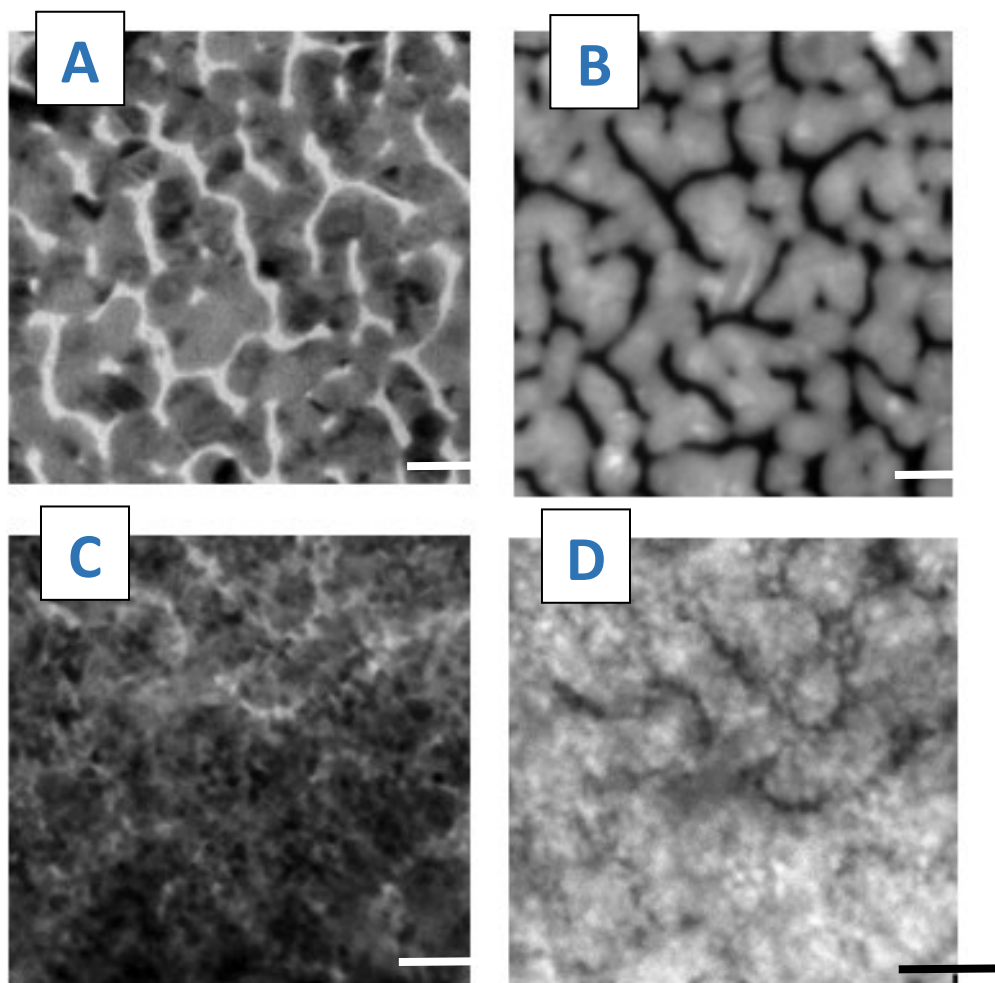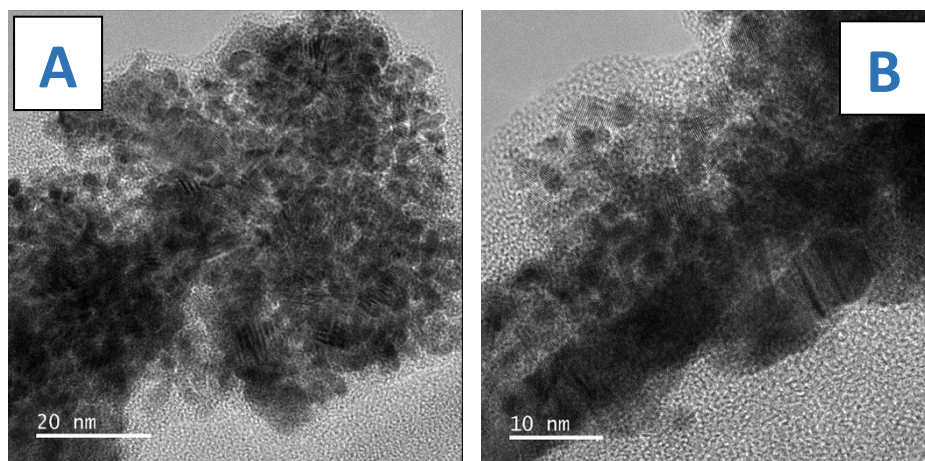
**Figure S5**

STEM bright field (left) and HAADF (right) images of Au/C (A, B) and C/Au/Pt nanostructureds deposited on ultrathin (ca 50 nm) nafion film on carbon grid support. Scalebars – 10 nm.
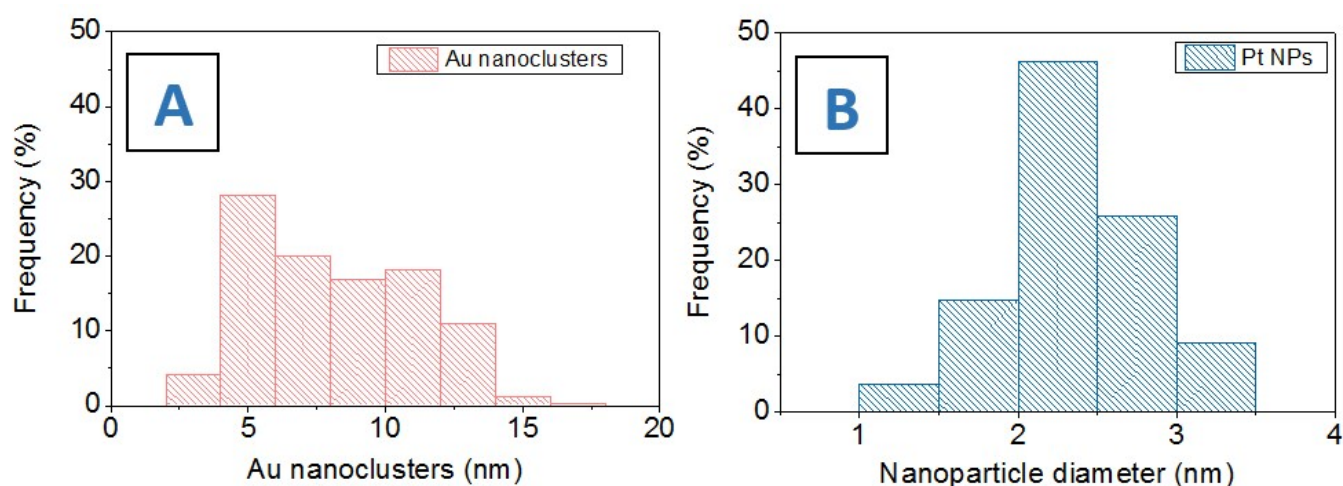
\

**Figure S6**

TEM bright field (A) and HRTEM (B) images of C/Au/Pt catalytic layer "scratched" from nafion support.



**Figure S7**

Size distribution histogram of Au (A) and Au/Pt (B) nanoclusters on PEM/C membrane calculated frpom TEM images.

**Table S1**

Results of control. BET measurements of surface area at the different stages of samples decoration with C, Au, and Pt.

| Sample | Surface area($m^2/g$) |
|---|---|
| Pristine PEM membrane | 67,6 ± 10,3 |
| PEM/C | 104,3 ± 8,2 |
| PEM/C/Au | 117,3 ± 7,2 |
| PEM/C/Au/Pt | 121,8 ± 4,5 |
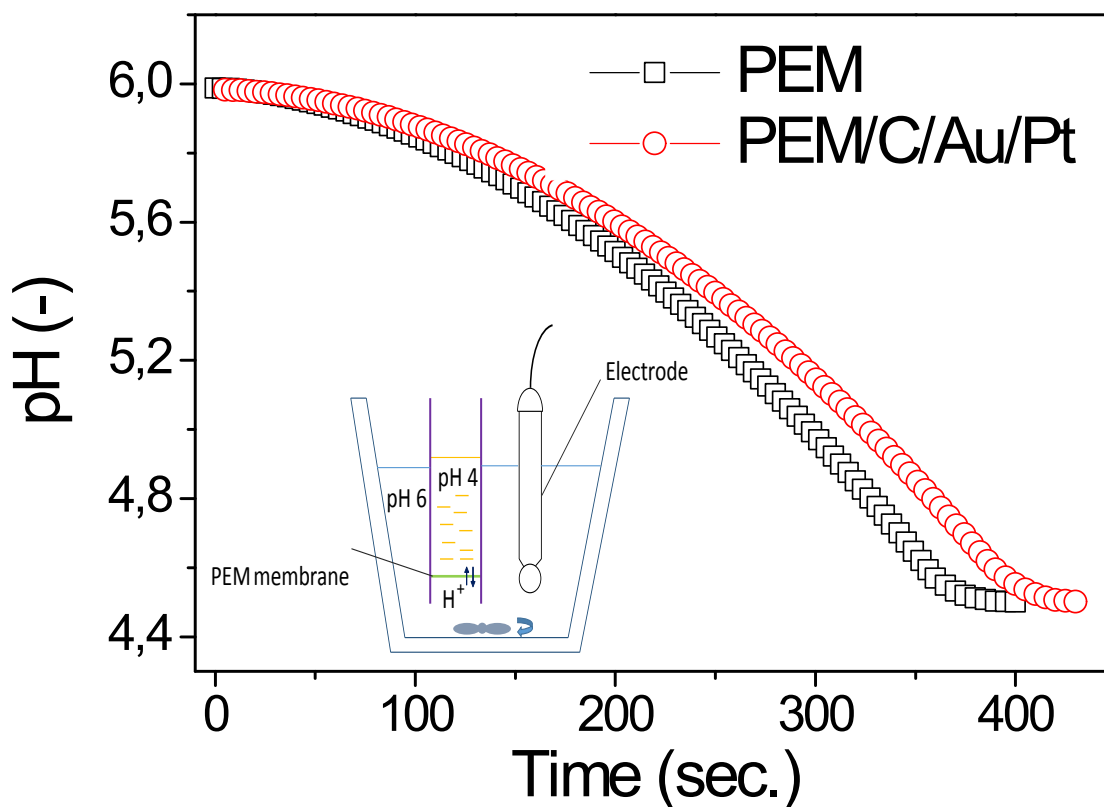
**Figure S8**

Schematic representation experimental arrangement (insert) and results of the proton conductivity measurement on . pristine PEM membrane vs PEM/C/Au/Pt membrane.
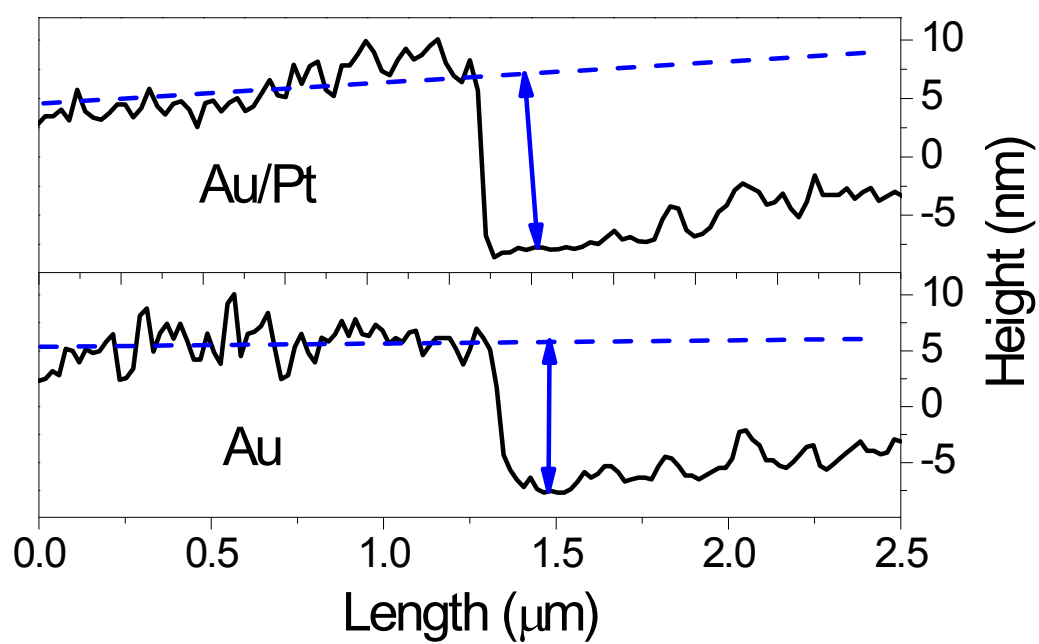
**Table S2** Surface chemical composition (in at %) measured by XPS at the different stages of PEM membrane surface decoration.

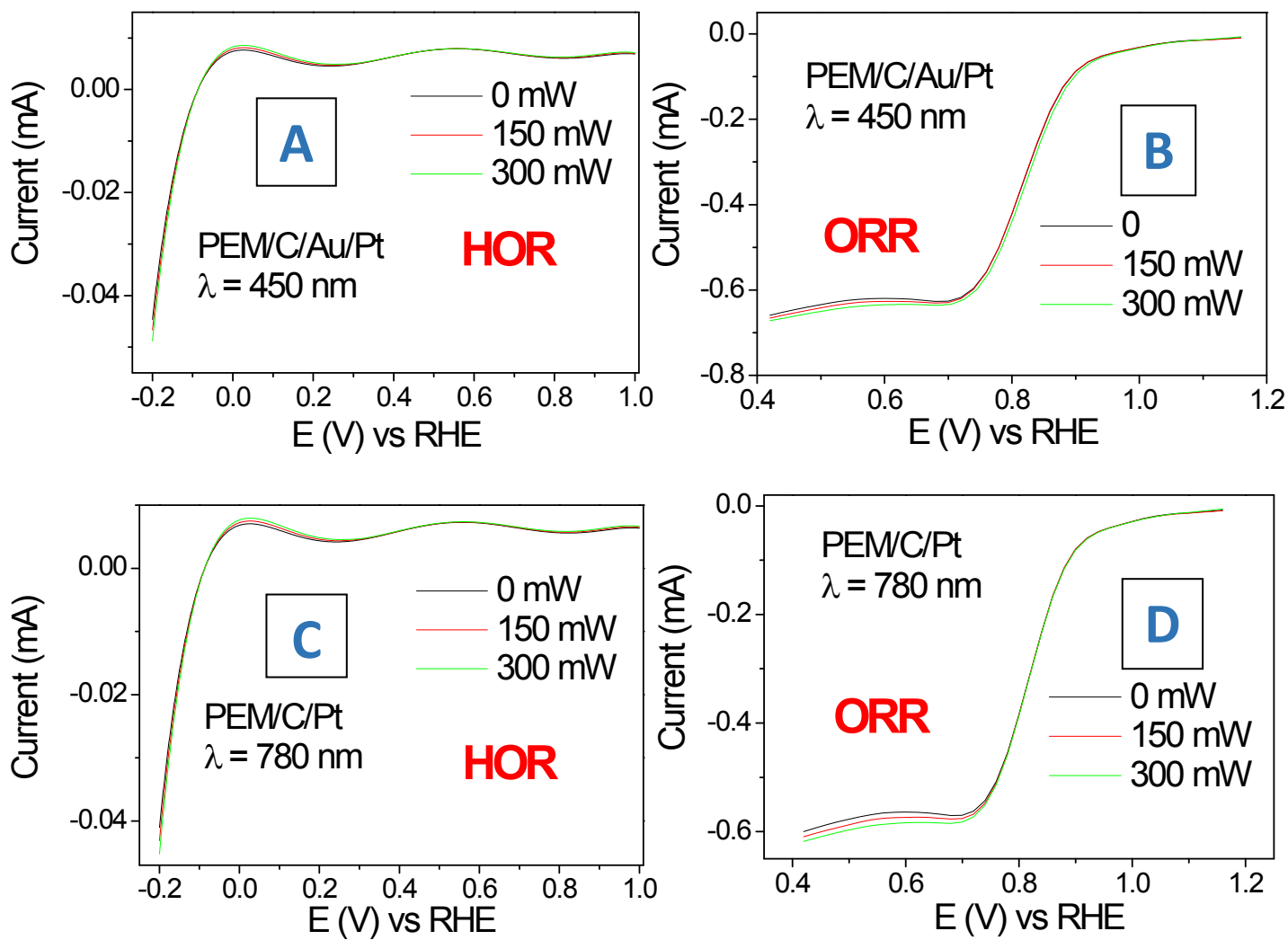| Samples | Elements (atomic %) | | | | | | |
|---|---|---|---|---|---|---|---|
| | C | O | F | S | Au | Pt | Cl |
| PEM | 38.1 | 8.2 | 52.3 | 1.4 | – | – | |
| PEM/C | 60.3 | 4.8 | 34.7 | 0.2 | – | – | |
| Au/C/Nafion | 43.7 | 5.1 | 24.6 | – | 26.6 | – | |
| Pt/Au/C/Nafion | 39.7 | 7.2 | 19.1 | – | 18.5 | 15.4 | 0.1 |
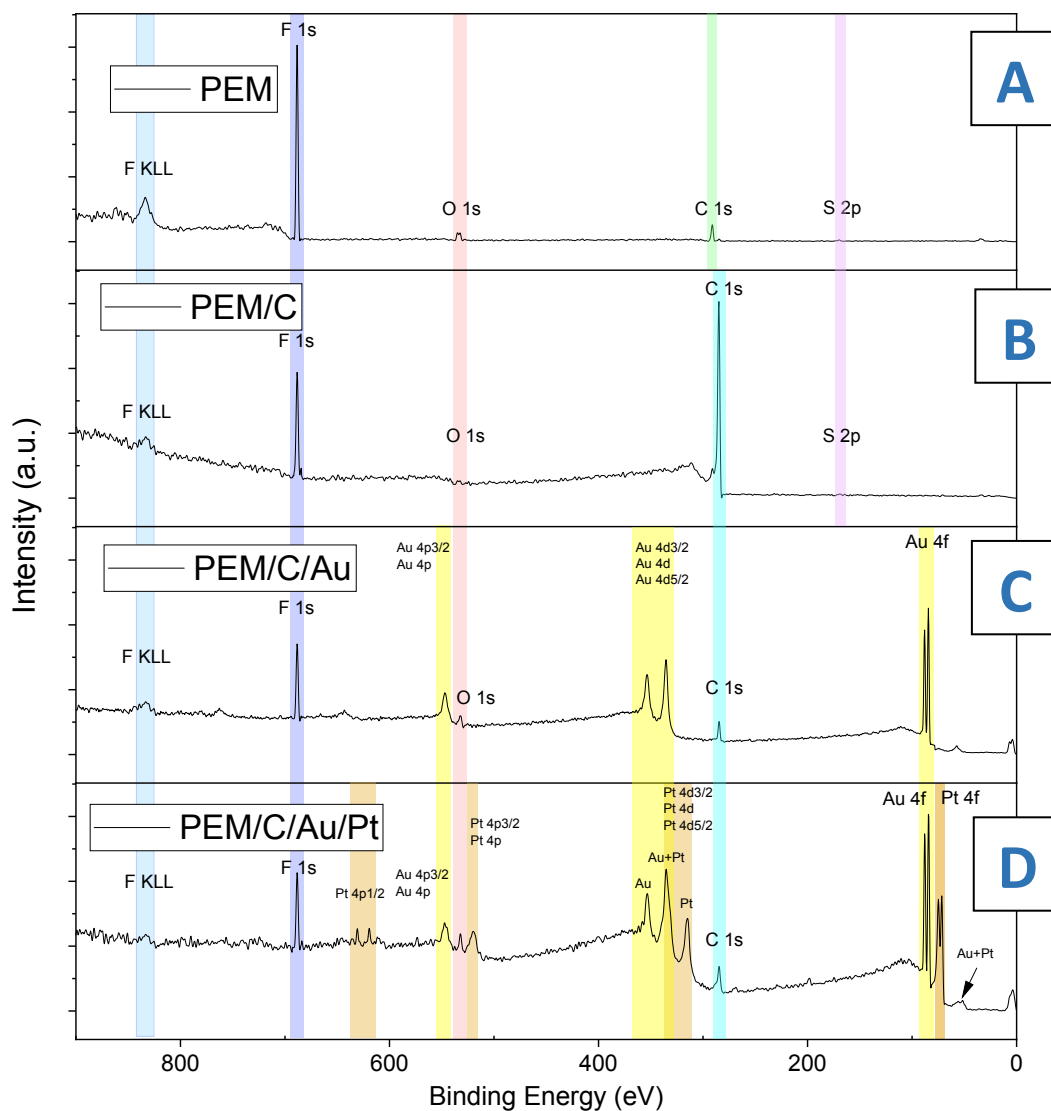
**Figure S9**

XPS spectra measured on pristine PEM membrane and PEM membrane with additional layers of C (B), Au (C), and Pt (D).
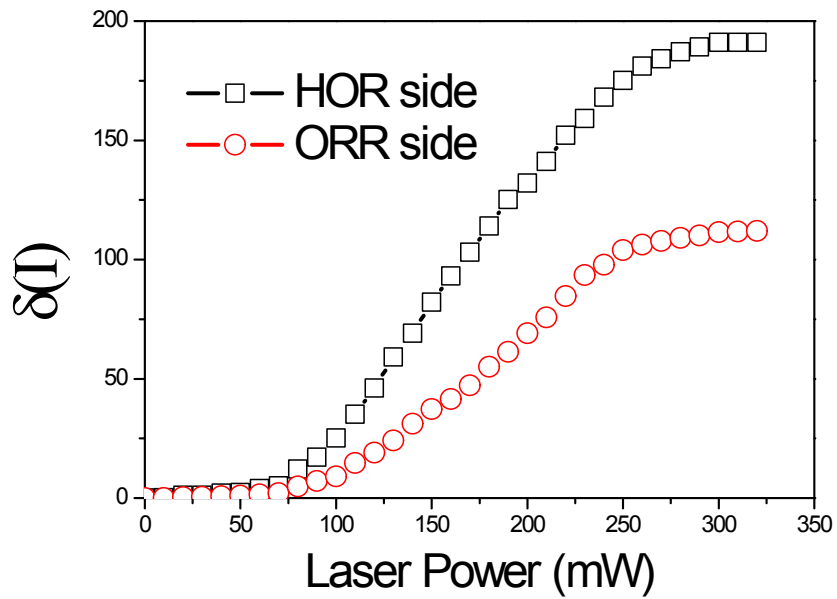
**Figure S10**

Results of AFM scratch test – determination of Pt thickness and loading.

**Figure S11**

Voltammetry control measurements, performed under the illumination with 450 nm wavelength (A, B) or without addition of plasmon active Au coating (C, D) with implementation of HOR and ORR model half-reactions.
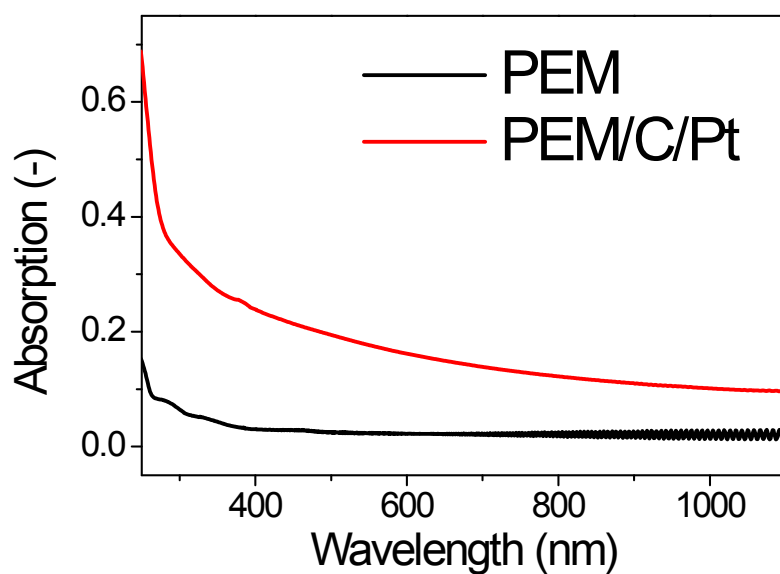
**Figure S12**

Produced electric current as a function of laser power under the plasmon triggering, applied alternatively on different sides of PEM/C/Au/Pt membrane, (sides responsible for HOR or ORR half-reactions).
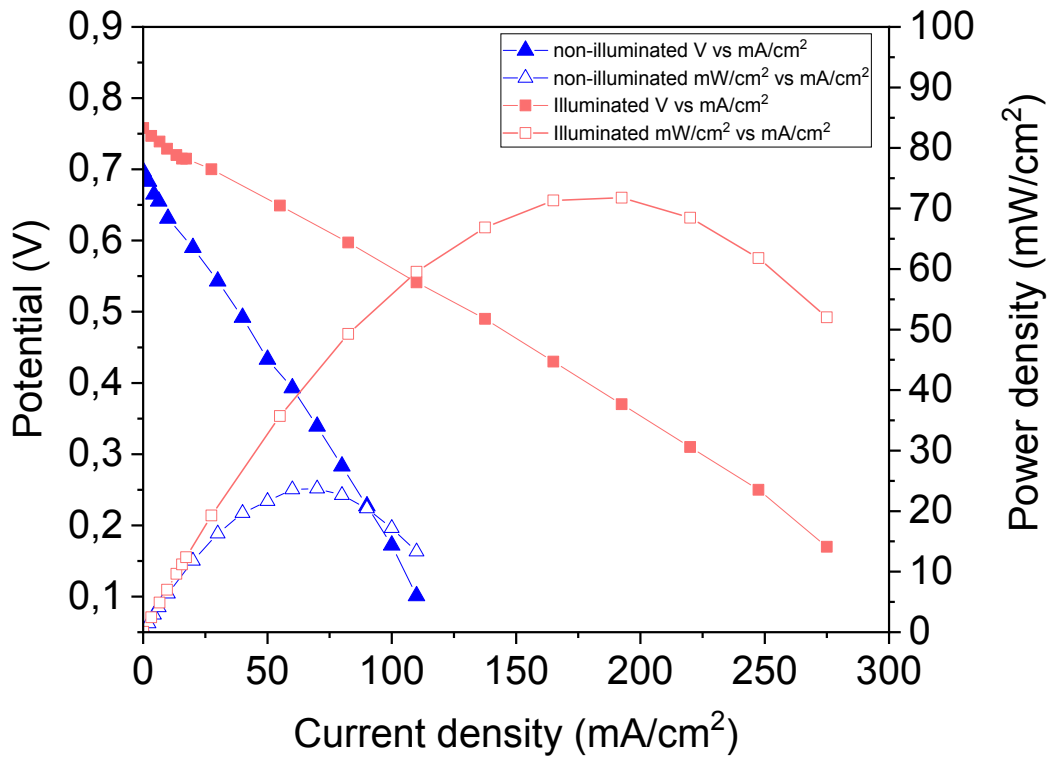


**Figure S13**

Polarization curves and power density curves measured in dark and under illumination (780 nm, 30 mW) of fuel cell with C/Au/Pt catalytic layer deposited on PEM membrane.



**Figures S14**

UV-Vis spectra of PEM coated by C and Pt (without addition of Au)